Gaia DPAC

Data Processing & Analysis Consortium

A generic LSF/PSF model and its role in IDT, FL, IDU and AGIS

prepared by: L. Lindegren
affiliation : Lund Observatory
approved by:
reference: GAIA-C3-TN-LU-LL-089-01
issue: 01
revision: 0
date: 2010-11-03
status: Issued

Abstract

This note defines generic LSF and PSF models and describes how the models are related to other processes, in particular the LSF and CDM calibrations in FL, IDU, and AGIS and the use of the LSF model in IDT.

Document History

Issue	Revision	Date	Author	Comment
D	0	2010-10-10	LL	Creation and 1st draft
1	0	2010-11-03	LL	Comments by CF and BAS incorporated

1 Introduction

The concept of a Line Spread Function (LSF) is fundamental for the astrometric and photometric processing of (one-dimensional) Gaia data. The importance of the concept derives from two circumstances. First, when dealing with unresolved point sources, LSF fitting is the most accurate way to estimate the location and flux, and the maximum accuracy is obtained when the correct LSF is used. Secondly, when dealing with more complex sources, in particular double and multiple stars, their disentanglement, if at all possible, necessarily relies on the linear superposition of the component LSFs. In both cases, LSF fitting allows to recognize bad samples, e.g., as caused by cosmic rays or saturation, which is not possible without an accurate LSF to compare with. The Point Spread Function (PSF) has the corresponding role for two-dimensional images.

The complete modelling of the CCD signal in terms of the astronomical stimulus contains many other elements besides the LSF, including the geometric and photometric properties of the instrument, and various non-linear properties of the detector (saturation, CTI effects, noise, ...) that cannot be accounted for in the LSF. This is illustrated in Fig. 1, where the LSF model (or PSF, in the case of two-dimensional CCD data) occupies the middle box. It is preceded by the geometric and photometric instrument models, which predict the location and flux[1] of the image in the CCD data stream, and followed by the Charge Distortion Model (CDM) and other model components representing the response of the CCD and output electronics to the expected photon counts. The important point to emphasize here is that the exact boundaries between the three middle boxes in Fig. 1 are, to some extent, arbitrary and must be fixed by convention. As the boxes typically represent distinct tasks in the processing chain, the adopted conventions partially determine *where* in the processing chain the different effects are taken into account. The boundaries need not be the same at all stages of the processing, as long as they are explicit and well-defined; for example, they could differ between the IDT, FL and IDU tasks.

The aim of this note is to summarize, as completely and consistently as possible, current thinking about the role of the LSF model in the various processes, with special regard to the definition of boundaries. When necessary, a clarification of the relevant conventions is proposed. For completeness, some basic definitions and relations concerning the LSFs and PSFs have been gathered in Sect. 2.

Many of the concepts discussed here have developed and changed quite a lot over a number of years. As a consequence, some previously introduced (and sometimes adopted) conventions may have become obsolete or superseded.

---

[1] 'Flux' is here taken to mean the total number of detected photons in a CCD observation of a source.
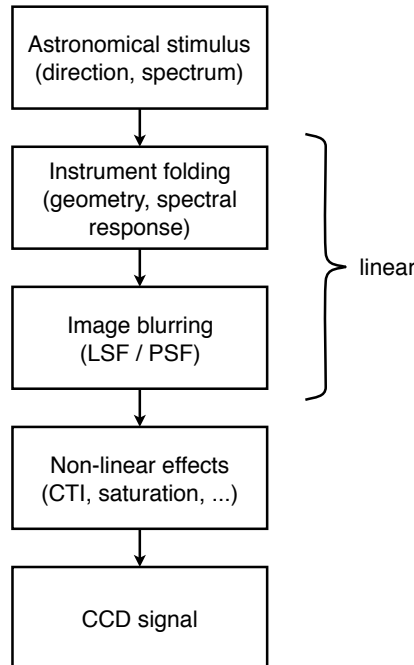
FIGURE 1: Schematic illustration of the various elements that fold into the CCD data model of an astronomical source. The exact boundaries between the middle three boxes must be fixed by convention.

2 Some basic definitions and conventions

A number of technical notes have discussed the relevant definitions, terminology and conventions related to the LSF/PSF, but since they are scattered among different documents and some of them have changed over time, it may be convenient to summarize the most important ones here.

2.1 Optical and effective LSF/PSF

An important first thing to note is that the LSF and PSF used in the Gaia data processing are always the *effective* LSF and PSF,[2] in the sense introduced by Anderson & King (2000). That is, the LSF and PSF take into account the pixellated nature of the image, as well as the additional image smearing caused by the TDI operation, speed mismatch during integration, and some other effects including the charge diffusion (electronic MTF). The important consequence of this convention is that the expected number of photons detected in sample k, from a single star located at κ, is proportional to $L(k - \kappa)$, if $L(u)$ is the (effective) LSF (cf. Fig. 2). Thus the integration over the nominal pixel width ($10~\mu$m) is implicitly included in the LSF.

[2]Sometimes (but not here) abbreviated eLSF and ePSF.

Similar considerations apply to the (effective) PSF, which thus includes the integration over the nominal pixel area (10×30 μm^2) and the AC charge diffusion, in addition to the AL effects already included in the LSF. The PSF is a function of u and the corresponding AC offset $v = m - \mu$, where m is the across-scan pixel coordinate of the pixel (an integer) and μ the across-scan pixel coordinate of the image. However, since the across-scan motion of the image during the CCD integration is highly variable and may be very significant (up to 4.5 pixels) we must in practice regard the effective PSF also as a function of the AC motion s (see Sect. 4 for details) which we write $P(u, v|s)$. Thus, the expected number of photons detected in pixel (k, m) from a single star located at (κ, μ) is proportional to $P(k - \kappa, m - \mu|s)$, where s is the (known) AC motion of the image during the integration (in pixels).

By contrast, the *optical* LSF $L_O(u)$ and PSF $P_O(u, v)$ describe the instantaneous one- and two-dimensional intensity distributions in the image falling on the CCD. The theoretical relation between the optical and effective spread functions is a convolution, which includes a rectangular boxcar function Π of unit width (since u and v are expressed in pixels):

$$L = L_O * \Pi_1 * S_1 \qquad \text{and} \qquad P = P_O * \Pi_2 * S_2 \,, \tag{1}$$

where $*$ is the convolution operator,

$$\Pi_1(u) = \begin{cases} 1 & \text{if } |u| < \frac{1}{2} \\ 0 & \text{otherwise} \end{cases} \qquad \text{and} \qquad \Pi_2(u, v) = \Pi_1(u)\Pi_1(v) \tag{2}$$

account for the pixelization, and $S_1(u)$, $S_2(u, v)$ account for the additional smearing effects mentioned above.

2.2 Normalization and sum-invariance of the LSF and PSF

Both the LSF and the PSF are by definition normalized to unit area and volume, respectively:

$$\int_{-\infty}^{+\infty} L(u) \, \mathrm{d}u = 1 \qquad \text{and} \qquad \iint_{-\infty}^{+\infty} P(u, v|s) \, \mathrm{d}u \, \mathrm{d}v = 1 \tag{3}$$

for any s. Since the boxcar functions in Eq. (2) have unit area/volume, it follows that also $L_S = L_O * S_1$ and $P_S = P_O * S_2$ are similarly normalized. An important consequence of Eq. (1) is then that (effective) LSF and PSF functions should obey the sum-invariance rule,

$$\forall \kappa, \mu: \qquad \sum_k L(k - \kappa) = 1 \qquad \text{and} \qquad \sum_k \sum_m P(k - \kappa, m - \mu|s) = 1 \,, \tag{4}$$

where the sums are taken over all integers k and m.

For the LSF, the sum-invariance is shown as follows: The convolution operator being associative and commutative, we have $L = \Pi_1 * L_S$. Then, for arbitrary κ,

$$\sum_k L(k - \kappa) = \sum_k (\Pi_1 * L_S)(k - \kappa) = \sum_k \int_{k - \kappa - \frac{1}{2}}^{k - \kappa + \frac{1}{2}} L_S(u) \, \mathrm{d}u = \int_{-\infty}^{+\infty} L_S(u) \, \mathrm{d}u = 1 \,, \tag{5}$$

since L_S is normalized. The sum-invariance of the PSF is shown in an analogous way.

In physical terms, the sum-invariance means that the total expected number of detected photons in a stellar image is invariant with respect to the sub-pixel position of the image, if the counts are summed over a sufficiently large window. This is a good approximation for back-illuminated CCDs, where the microscopic quantum efficiency is practically independent of sub-pixel position. It is important that the LSF/PSF model is also sum-invariant, in order to avoid introducing artificial biases, as function of sub-pixel position, in the fitting process.

2.3   Relation between the LSF and PSF

In standard (non-Gaia) image science, the LSF is defined simply as the marginal density of the PSF: $L(u) = \int_{-\infty}^{+\infty} P(u, v) \, dv$. For Gaia, the corresponding relation reads $L(u) = \int_{-\infty}^{+\infty} P(u, v|s) \, dv$, valid for any s. A practical difficulty with this definition is that for the vast majority of observations, only a finite range in the AC coordinate (v) is observed, usually a window of $M = 12$ pixels. A convention has therefore been adopted, namely that the LSF is obtained by considering only the central part of the PSF in the AC direction, corresponding to the most commonly used AC window. More precisely, the following convention is proposed here:

$$L(u) = C(0|0) \sum_{m=0}^{M-1} P\left(u, m - \tfrac{M-1}{2}|0\right) , \tag{6}$$

where $C(0|0)$ is the normalization factor (slightly larger than 1) required by Eq. (3a):

$$C(0|0) = \left[\int_{-\infty}^{+\infty} \sum_{m=0}^{M-1} P\left(u, m - \tfrac{M-1}{2}|0\right) \, du \right]^{-1} . \tag{7}$$

Note that the relation between the LSF and PSF must be defined in terms of a *sum* over the M AC pixels, rather than an integral over the continuous AC coordinate, $-M/2 < v < M/2$, and that we have chosen to use the PSF with $s = 0$ for this convention. Introducing the AC LSF

$$L_{\mathrm{AC}}(v|s) = \int_{-\infty}^{+\infty} P(u, v|s) \, du \tag{8}$$

we could more generally define

$$C(v|s) = \left[\sum_{m=0}^{M-1} L_{\mathrm{AC}}\left(v + m - \tfrac{M-1}{2}|s\right) \right]^{-1} \tag{9}$$

as the correction required when the PSF is offset by v pixels in the AC direction from the centre of the window and has the AC smearing s. The (slight) variation of the LSF shape with v and s is here ignored.
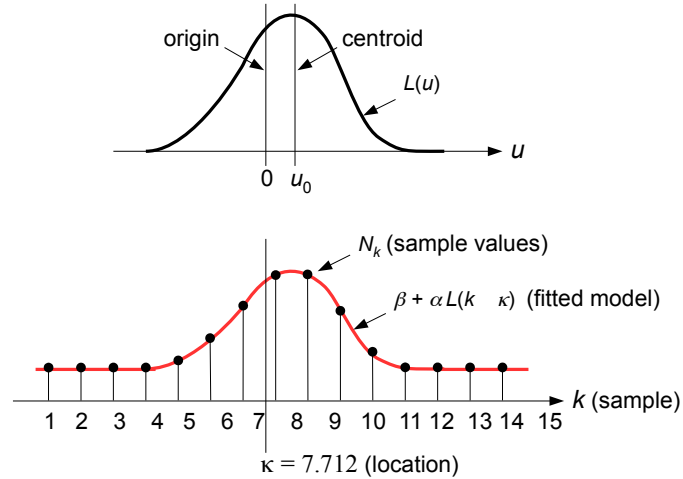
FIGURE 2: Definition of centroid, origin and location: the top diagram shows a schematic LSF with the origin ($u = 0$) and centroid ($u = u_0$) indicated. The bottom diagram shows the location (κ) of the LSF in the stream of sample values N_k. In this case the scene consists of a uniform background of brightness β (in electrons per sample) plus a single point source of intensity α (in electrons) at $k = \kappa$.

As a consequence of these relations, the LSF fitting only compensates for the flux outside the window in the AL direction, while the PSF fitting compensates for all flux outside the window.

That is, when fitting $\beta + \alpha P(k - \kappa, m - \mu | s)$ to a two-dimensional image, the resulting flux estimate α refers to the total flux of the image, including all parts outside the sampled window. However, when $\beta + \alpha L(k - \kappa)$ is fitted to a one-dimensional image, the resulting flux estimate α only refers to the flux within the AC interval $m = 0 \ldots M - 1$, and therefore requires a correction by the factor $C(v|s)$ to represent the full flux, where v is the offset in AC and s the amount of AC smearing.

2.4 Centroid, origin and location

A clear distinction between these three terms was introduced in Lindegren (LL-080), from which Fig. 2 is taken. Briefly, with reference to the LSF $L(u)$ schematically shown in Fig. 2,

- the *centroid* u_0 is defined by the shape of the LSF itself without any reference to external data. For a symmetric LSF it is naturally given by the point of symmetry, but for more general shapes it is necessary to introduce some convention for the definition of the centroid. This is further discussed below;

- the *origin* is the agreed reference point where $u = 0$. It could be the centroid, but in general it is not (i.e., $u_0 \neq 0$ in general). The main reason for this is chromatic-

ity: the origin should correspond to a well-defined point on the celestial sphere, independent of the colour of the source. This is further discussed in Sect. 6.2;

- the *location* is the coordinate (or coordinates, for a PSF) of the origin in the fitted image, i.e., in the CCD sample stream. It may be given as a pixel coordinate, as in Fig. 2, or (in the AL direction) converted to the corresponding 'transit time' when the origin passes to the serial register, or to the 'observation time' when the origin passes the fiducial observation line close to the centre of the integration.

Concerning the definition of the centroid u_0 of the arbitrary LSF $L(u)$, several different conventions have been proposed and used over the years, including 'the minimum difference mirror point' (Lindegren, GAIA-LL-044), minimizing

$$\int_{-\infty}^{+\infty} \left[L(u_0 + x) - L(u_0 - x) \right]^2 \, \mathrm{d}x \,, \tag{10}$$

and a family defined in terms of some odd analytical weighting function $w(x)$, such that

$$\int_{-\infty}^{+\infty} L(u_0 - x) w(x) \, \mathrm{d}x = 0 \,, \tag{11}$$

where in particular the weighting function representing Tukey's biweight (TBW) was advocated in Lindegren (LL-068).

The precise definition of the centroid is unimportant for the following discussion, as long as a well-defined prescription exists. However, in the context of the generic LSF model described in Sect. 3, it appears that the most natural definition is simply the origin of the adopted basis functions, i.e., $u_0 = h_0$.[3]

3 A generic LSF model

3.1 General formulation

In Lindegren (LL-088), the following very general representation of the LSF in terms of basis functions $H_n(x)$ was introduced:

$$L(u) = \begin{cases} H_0(u - h_0) + \sum_{n=1}^{N-1} h_n H_n(u - h_0) & \text{if } N > 0 \,, \\ H_0(u) & \text{otherwise.} \end{cases} \tag{12}$$

The model, here referred to as the *generic LSF model*, depends on $N \geq 0$ model parameters. The case $N = 0$ corresponds to a 'default' LSF equal to $H_0(u)$, while for $N > 0$ the model

---

[3]In general this origin does not coincide with the mirror point or TBW centroid, except for symmetric profiles. Moreover, it does not exactly correspond to the point obtained by fitting H_0 to the profile, except when the profile is symmetric.

parameters are h_n, $n = 0, \ldots N - 1$. The default LSF, which may be used in the absence of any other information, should ideally be close to the expected (mean) LSF of the real instrument. Moreover, the default value of any parameter is $h_n = 0$, so that the default LSF is also obtained by putting all parameters equal to zero. The first parameter h_0 represents a pure shift of the origin of the LSF.

The basis functions must satisfy

$$\int_{-\infty}^{+\infty} H_n(x) \, \mathrm{d}x = \delta_{0n} \tag{13}$$

for all n, where δ_{ij} is Kronecker's delta. This guarantees that $L(u)$ is normalized to unit area for any choice of model parameters. The sum-invariance property of the LSF is satisfied if, in addition, all the basis functions have the corresponding property,

$$\forall \kappa : \qquad \sum_k H_n(k - \kappa) = \delta_{0n} \, . \tag{14}$$

Apart from the strict constraints in (13), the basis functions should satisfy some less well-defined criteria, viz.:

1. The basis functions are such that the linear combination in (12) can represent any observed LSF to sufficient accuracy. This requires a certain minimum number of basis functions to be defined, spanning the relevant subspace of possible LSFs.

2. H_0 is not far from the mean actual LSF over some relevant set of LSFs, as discussed above.

3. The basis functions of increasing order $n = 1, 2, \ldots$ represent ever finer details of the LSF, so that a truncated expansion provides a useful approximation of the full expansion.

4. The basis functions are approximately orthogonal.

5. The derivative $H_0'(x)$ does not belong to the linear subspace spanned by the basis functions.

The first criterion is obviously necessary for the model to be at all useful; however, it is not easily quantified as a requirement, if only because the relevant set of LSFs is not known beforehand. The second and third criteria are related to the desired property that we want to use as few free parameters as possible to model the observed LSFs. The fourth criterion ensures numerical stability of the fitting process. The fifth criterion ensures that the shift parameter h_0 is not degenerate with respect to the other parameters.

3.2 Interface

The interface to the generic model is very simple. On construction, a default LSF (equal to H_0) is set up, equivalent to $N = 0$ model parameters. Methods are needed to set the number and values of the parameters (h_n, $n = 0, 1, \ldots N - 1$), and to get the function value $L(u)$ and its derivative $L'(u)$ for arbitrary argument u, as well as the N partial derivatives $\partial L / \partial h_n$ for arbitrary u.

$L(u)$ and $L'(u)$ are generally needed for the image parameter determination. $L(u)$ and $\partial L / \partial h_n$ may be needed for the LSF calibration, but not for the image parameter determination.

3.3 Implementation: LSF88

Within this general framework one can in principle define many different sets of basis functions $\{H_n(x)\}$ that might work about equally well for the real LSFs of Gaia. One example is given in Lindegren (LL-088), based on the Principal Component Analysis (PCA) in Lindegren (LL-084) of a large ensemble of randomly generated, but physically plausible LSFs. This set of basis functions, using components up to $n \simeq 50$, has been found to fit (and, indeed, overfit) all observed undamaged LSFs in several sets of astrometric test data from Radiation Campaign #3 and #4 (C. Crowley). In the following I will refer to this particular implementation of the generic LSF model as the LSF88 model. However, all subsequent discussion of the LSF model and its role in IDT, FL, IDU and AGIS refers to the generic model and is not directly linked to LSF88.

Nevertheless, LSF88 appears to provide a sufficiently accurate and flexible model to work in all current and planned simulations, and perhaps even as a starting approximation in the real Gaia data processing. Lindegren (2010) describes a procedure whereby the basis functions can later be redefined in the light of the real data. Figure 3 shows the first four basis functions in LSF88, while Fig. 4 shows what the LSF looks like when the first four parameters take the values -1, 0 and $+1$. As already mentioned, h_0 represents a shift of the origin, and it is seen that h_1 mainly affects the width of the LSF, h_2 the skewness, and h_3 the kurtosis of the LSF. The details of these curves depend of course on the precise definition of basis functions, but it is reasonable to expect that *any* set of basis functions that satisfy all the criteria listed above will look somewhat similar in its lowest orders, with in particular h_1, h_2, and h_3 representing modifications of the width, skewness and kurtosis relative to the default LSF.
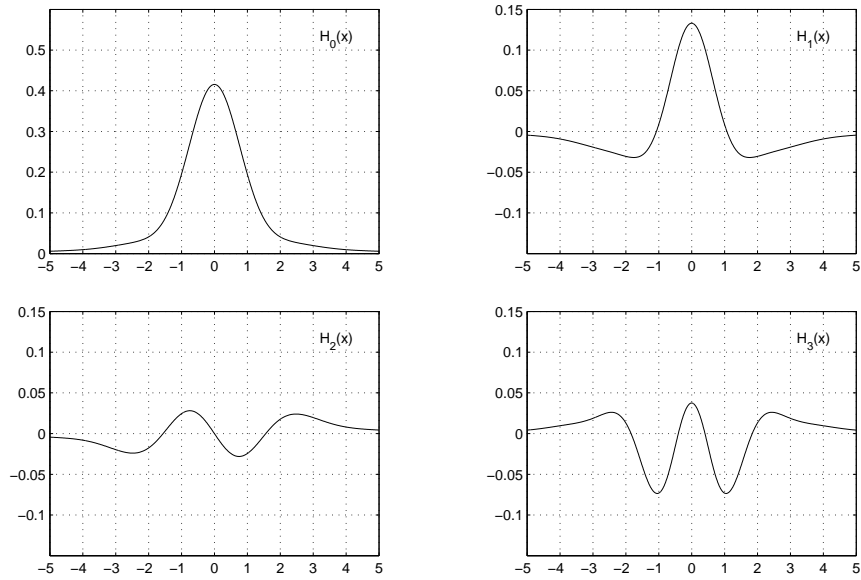
FIGURE 3: The first four basis functions $H_n(x)$, $n = 0 \ldots 3$, in the LSF88 model, i.e., the generic model as implemented in Lindegren (LL-088).
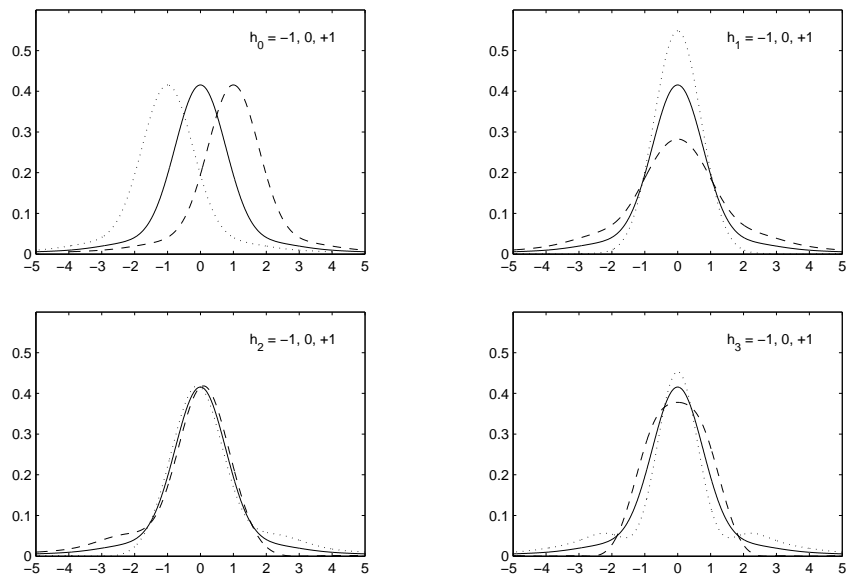
FIGURE 4: The LSF as described by the LSF88 model, when the first four parameters h_n, $n = 0 \ldots 3$ take the values -1 (dotted curves), 0 (solid curves), and $+1$ (dashed curves).

3.4 Modification for binned data

SM data are binned 2×2 or 4×4 pixels, which drastically modifies the LSF and PSF. The generic model can easily take this into account, without necessarily redefining the basis functions; however, the normalization issues should be carefully considered and adopted conventions clearly defined.

Consider the AL binning by 2 pixels as an example. If the 2-binned LSF is defined as

$$\bar{L}(u) = L(u - \tfrac{1}{2}) + L(u + \tfrac{1}{2}), \tag{15}$$

the expected number of electrons in a sample from a source with flux α is $N_k \sim \alpha\bar{L}(k - \kappa)$ for $k \in K$, where K is the set of pixel coordinates for the binned samples (e.g., the even integers). This LSF satisfies the normalizations[4]

$$\int_{-\infty}^{+\infty} \bar{L}(u)\,\mathrm{d}u = 2 \qquad \text{and} \qquad \forall\kappa: \quad \sum_{k\in K} \bar{L}(k - \kappa) = 1. \tag{16}$$

The generic model for the 2-binned LSF is

$$\bar{L}(u) = \bar{H}_0(u - h_0) + \sum_{n=1}^{N-1} h_n \bar{H}_n(u - h_0), \tag{17}$$

where the 2-binned basis functions are correspondingly defined in terms of the unbinned basis functions:

$$\bar{H}_n(x) = H_n(x - \tfrac{1}{2}) + H_n(x + \tfrac{1}{2}). \tag{18}$$

In the LSF88 implementation, the binned basis functions can be represented (to sufficient approximation) in the same manner as the unbinned basis functions, i.e., as a sum of a biquartic spline and an analytical tail, only with a different set of coefficients; in this way the evaluation of the binned LSF will not require more operations than the unbinned LSF.[5]

The use and calibration of the binned LSF model is therefore completely analogous to the unbinned version, and the physical interpretation of the model parameters h_n is in fact independent of the binning. This means that the same set of parameters can be used for, and even calibrated from, any mixture of binned and unbinned data.

The extension of the above to arbitrary binning factors in AL and AC is trivial.

---

[4]Obviously it is just a matter of convention where to put the factor 2 (or $1/2$) in these equations; an alternative convention could be $\bar{L}(u) = \tfrac{1}{2}[L(u-\tfrac{1}{2})+L(u+\tfrac{1}{2})]$ with $N_k \sim 2\alpha\bar{L}(k-\kappa)$ and the normalizations $\int_{-\infty}^{+\infty} \bar{L}(u)\,\mathrm{d}u = 1$ and $\sum_{k\in K} \bar{L}(k - \kappa) = \tfrac{1}{2}$.

[5]The binned biquartic spline is another biquartic spline obtained by binning the coefficients; the binned tail function can well enough be approximated by 2 times the same tail function.

4 A generic PSF model

As previously discussed, the PSF model must allow a variable amount a smearing $s \geq 0$ in the AC direction due to AC image motion during the integration. A possible generic PSF model, obtained by an obvious two-dimensional extension of the generic LSF model, is

$$P(u, v|s) = H_0(u - h_0)K_0(v - v_0|s) + \sum_{\substack{n=0 \\ n+j>0}}^{N-1} \sum_{j=0}^{J-1} h_{nj}H_n(u - h_0)K_j(v - v_0|s), \qquad (19)$$

where $\{K_j(y|s)\}$ is a set of basis functions for the AC LSF with a similar normalization as in Eq. (13). The parameters are h_0, v_0, and h_{nj} for $n = 0 \ldots N - 1$ and $j = 0 \ldots J - 1$, excluding h_{00}, i.e., in total $NJ+1$ parameters. However, not all $NJ+1$ need to be defined (the remaining ones being 0 by default); for example, retaining only h_{0j} and h_{n0} is equivalent to a PSF that is the product of the corresponding LSFs in the AL and AC directions.

For each observation the amount of smearing in the AC direction, s (pixels), is a known quantity and its effect on the PSF can be described by a rectangular convolution. The basis functions $K_j(y|s)$ for $s > 0$ can therefore be defined in terms of $K_j(y|0)$ as

$$K_j(y|s) = \frac{1}{s} \int_{-s/2}^{+s/2} K_j(y - t|0) \, \mathrm{d}t \,. \qquad (20)$$

For $K_j(y|0)$ we may use a similar set as $H_n(x)$, but the efficient implementation of Eq. (20) remains to be worked out and will depend on the mathematical representation of $K_j(y|0)$.

The important point to note is that the PSF parameters h_0, v_0 and h_{nj} in Eq. (19) are *not* affected by the AC smearing. Thus they can be calibrated from a set of observations with varying degree of AC motion, as long as the relevant s is used when computing the expected photon counts in each observation. The s applicable to each observation is of course known from the attitude and geometric calibration.

The AC LSF is readily obtained by applying the integral in Eq. (8) to (19) and using (13); the result is

$$L_{\mathrm{AC}}(v|s) = K_0(v - v_0|s) + \sum_{j=1}^{J-1} h_{0j}K_j(v - v_0|s), \qquad (21)$$

from which the photometric correction factor $C(v|s)$ can be calculated as in Eq. (9) as a function of the AC offset v and smearing s.

5 Two approaches to the LSF calibration

In terms of the generic LSF model, the LSF calibration simply means that the parameters h_n, $n = 0 \ldots N - 1$, are estimated from a given set of one-dimensional images $\{N_k\}$ (where we can

assume that the background has been subtracted). In the general case, this estimation is made via the Charge Distortion Model (CDM), in order to take into account radiation damage effects. However, for the discussion in this section we disregard all complications caused by the CTI, i.e., we assume that the counts are unaffected by radiation damage.

In order to clarify the relations between the LSF calibration and AGIS, two different approaches to the LSF calibration will be described below. They are referred to by the terms *internal* and *total* LSF calibration. [6] While the total LSF calibration determines all the LSF parameters in a single process, the internal calibration leaves certain LSF parameters (viz., h_0) undetermined, or set to zero.

5.1   Internal LSF calibration

The input to this procedure consists of the background-subtracted sample data $\{N_{ik}\}$ for each of the calibration images i, and nothing else. It proceeds roughly by the following steps:

1. For each image, the location κ_i of the centroid is estimated by some suitable procedure, e.g., by maximizing the cross-correlation with $H_0(x)$. Each sample is assigned the coordinate $x_{ik} = k - \kappa_i$.

2. The counts of each image are flux-normalized: $\hat{N}_{ik} = N_{ik}/\sum_k N_{ik}$ (possibly with a correction factor for the flux outside of the window in the AL direction).

3. The LSF parameters h_n, $n = 0 \ldots N - 1$, are fitted to the full data set $(x_{ik}, \hat{N}_{ik})$ using least-squares, chi-square minimization or maximum likelihood.

4. The shift parameter h_0 is set to zero.

5. The procedure may be iterated, as the provisional LSF generally allows to improve the estimated centroid and flux of each image.

Experience shows that it is not useful, and possibly harmful, to iterate the centroid and flux estimation more than once.

One can think of many variants of this procedure, in particular to make it more robust. For example, normalized counts can be grouped, according to $k - \kappa_i$, into bins that are much smaller than a pixel, and a robust normal point formed within each bin; the LSF model is then fitted to the normal points rather than to the original counts.

The important feature of the intrinsic LSF calibration is that it cannot determine a meaningful shift parameter h_0, which is why it is set to zero in Step 4. However, h_0 must be included as a free parameter in Step 3, since the centroiding in Step 1 does not necessarily correspond to $h_0 = 0$ (cf. footnote 3).

---

[6] 'Total calibration' is preferred to the perhaps more obvious choice 'external calibration', which rather implies a procedure to make the internal calibration total; cf. Sect. 6.

5.2 Total LSF calibration

In this process we need, in addition to the (background-subtracted) sample data $\{N_{ik}\}$, knowledge about the source, attitude, and (geometric) calibration parameters. Normally these are provided by a previous AGIS solution. The relevant information is combined in the *field angle offsets* (FAO)

$$D\eta(t) = \eta^{\mathrm{obs}}(\mu(t)|\boldsymbol{c}) - \eta^{\mathrm{calc}}(t|\boldsymbol{s}, \boldsymbol{a}, \boldsymbol{g}) \,, \tag{22}$$

$$D\zeta(t) = \zeta^{\mathrm{obs}}(\mu(t)|\boldsymbol{c}) - \zeta^{\mathrm{calc}}(t|\boldsymbol{s}, \boldsymbol{a}, \boldsymbol{g}) \,, \tag{23}$$

which are the computed offsets, along η (AL) and ζ (AC) of the image centre at time t from the relevant observation line.[7] $\boldsymbol{s}$, $\boldsymbol{a}$, $\boldsymbol{c}$ and $\boldsymbol{g}$ are source, attitude, calibration and global parameters calculated by AGIS. The calculation of the FAO can be regarded as a black box: it will be provided in GaiaTools and there is no need to understand how it actually works. The important thing to know is that for $t = t_{\mathrm{obs}}$ (the 'observation time' of the image, i.e., when the LSF origin passes the fiducial observation line of the CCD), we expect $D\eta = 0$. Thus, if we insert $t = t_{ik}$ (the observation time of sample ik) in the FAO calculator, the returned value $D\eta_{ik}$ is the calculated offset of the sample from the LSF origin. Dividing by the AL pixel size p_η (in radians) gives the calculated offset in pixels.[8]

The total LSF calibration then may proceed as the internal LSF calibration with two important modifications: the AL sample coordinate is calculated as $D\eta_{ik}/p_\eta$ instead of $k - \kappa_i$, and h_0 is retained. Thus:

1. For each image i, the FAO of one sample k (preferably near the centre of the image) is calculated and the sample is assigned the coordinate $x_{ik} = D\eta_{ik}/p_\eta$. The other samples in the image are assigned coordinates that differ by integer values from this ($x_{ik+1} = x_{ik} + 1$, etc).

2. The counts of each image are flux-normalized: $\hat{N}_{ik} = N_{ik}/\sum_k N_{ik}$ (possibly with a correction factor for the flux outside of the window in the AL direction).

3. The LSF parameters h_n, $n = 0 \ldots N - 1$, are fitted to the full data set $(x_{ik}, \hat{N}_{ik})$ using least-squares, chi-square minimization or maximum likelihood.

---

[7]$\eta^{\mathrm{obs}}(\mu|\boldsymbol{c})$ is called the 'observed' AL field angle, because we know that at the time of observation t_{obs} the image is located exactly on the fiducial observation line of the relevant FoV/CCD/gate combination, and $\eta^{\mathrm{obs}}(\mu|\boldsymbol{c})$ is the equation of this fiducial line as function of the AC pixel coordinate μ (depending on the geometric calibration parameters in $\boldsymbol{c}$). Similarly $\eta^{\mathrm{calc}}(t|\boldsymbol{s}, \boldsymbol{a}, \boldsymbol{g})$ is called the 'calculated' AL field angle, even though it *usually* (but not always!) is calculated for the observation time $t = t_{\mathrm{obs}}$. See Lindegren (LL-063) for some further discussion of the related terminology.

[8]It may not be immediately obvious that $D\eta_{ik}/p_\eta$ gives $k - \kappa_i$ with the correct sign. For the samples in a given observation, η^{obs} will be almost constant while η^{calc} will decrease with time. $D\eta$ will therefore increase with time as does also k by definition. Similarly, $D\zeta_{ik}/p_\zeta$ gives $m - \mu_i$ with the correct sign: for a given source at a given time, pixels at a higher column m will correspond to larger ζ, so ζ^{obs} will be larger while ζ^{calc} will be nearly constant. $D\zeta$ will therefore increase with m.

4. The procedure may be iterated to improve the estimated flux of each image.

5. Re-normalize the LSF calibration by subtracting the h_0 estimated for the reference SED (see Sect. 6.2).

In this case the LSF calibration provides a meaningful estimate of the shift parameter h_0. We will have $h_0 \neq 0$ if there are errors in the geometric calibration provided by AGIS, or because of chromaticity (e.g., different spectra give different h_0 for the same FoV/CCD/gate combination).

The total PSF calibration is analogous (see Sect. 7).

5.3 Comparing the internal and total LSF calibration

Although the two approaches to the LSF calibration use the same LSF model, the results are in general different. In particular, $h_0 = 0$ by definition for the internal calibration, while it may be non-zero for the total calibration. For the remaining LSF parameters h_n, $n > 0$, which describe the *shape* of the LSF, one should in principle obtain the same values in the two approaches. However, in practice one must expect significant differences due to the finite accuracy by which the sample coordinates x_{ik} are obtained:

- The (random) errors in x_{ik} result in a calibrated LSF that is slightly wider than the true LSF.

- For the internal LSF calibration, the errors in x_{ik} come from the sensitivity of the centroid estimation to the photon noise and RON of the individual image. These errors are independent of the AGIS solution but increase for faint stars.

- For the total LSF calibration, the errors in x_{ik} come from the errors in the source parameters, attitude, and geometric calibration, via the FAO calculation. These are expected to be relatively large in the early stages of the mission, and later decrease to a much lower level than for the internal LSF calibration, especially for the fainter stars.

Eventually, the total LSF calibration should be used, because it is expected to determine the LSF shape more accurately (once the source and attitude parameters are accurate enough) and because it gives a direct determination of the shift parameter needed for a correct treatment of chromaticity.

However, in the early stages of the mission it is probably much preferable to use the internal LSF calibration, as being less susceptible, e.g., to attitude errors. One must be aware of the possible side effects, for example that the LSF may appear systematically wider for the faint stars, and that AGIS may find a significant chromaticity.

It appears natural to use the internal LSF calibration in FL, and the total LSF calibration in IDU. For the image parameter determination, one can use either calibration both in IDT and IDU,

depending on what is available or which is the more reliable calibration at a certain stage. At an early stage of the mission, the IDU may benefit from using the internal calibration (optionally followed by an external calibration as discussed in Sect. 6.1). It is also quite possible that the selection may depend on brightness: at some stage, the internal calibration may be preferred for bright stars and the total for faint. The conclusion is therefore that both methods of calibration should be available in IDU, and that both IDT and IDU should be able to use either calibration for the image parameter determination.

Regarding the magnitude distribution of calibration stars, it should be recalled that we have only rather narrow ranges available for the gated observations. For the ungated observations, at least the PSF will also be obtained from certain narrow magnitude intervals (ungated bright stars, and Calibration Faint Stars). As far as gated, bright stars are concerned, saturation will be a concern.

6 External calibration and the role of AGIS

6.1 Chromaticity and CTI effects in AGIS

The generic calibration model for AGIS (Lammers, UL-031) allows to add terms in the functions $\eta_{\rm cal}$ and $\zeta_{\rm cal}$ of the FAO calculator that depend on quantities such as the effective wavenumber ($\nu_{\rm eff}$) and magnitude (G) of the source, and the time (T) since the previous charge injection. Typically, the complete AL calibration function may look something like this:

$$\eta_{\rm cal} = \eta_{\rm geo} + (\nu_{\rm eff} - \nu_{\rm ref})c_0 + \sum_{\alpha} \sum_{\substack{\beta \\ \alpha+\beta>0}} b_{\alpha\beta}\, g^{\alpha}\, \tau^{\beta}\,, \tag{24}$$

where $g = (G - G_{\rm ref})/5$ and $\tau = \log_{10}(T/T_{\rm ref})$ are suitably normalized variables for the magnitude and change injection delay. $\eta_{\rm geo}$ is the purely geometric part of the calibration, depending on a subset $\boldsymbol{c}_{\rm geo}$ of the calibration parameters; the non-geometric calibration parameters $\boldsymbol{c}_{\rm non}$ consist (in this example) of the parameters c_0 and $b_{\alpha\beta}$.

The reference values $\nu_{\rm ref}$, $G_{\rm ref}$, and $T_{\rm ref}$ have the following meaning: The purely geometric calibration $\eta_{\rm geo}$ is valid for an observation with $\nu_{\rm eff} = \nu_{\rm ref}$, $G = G_{\rm ref}$, and $T = T_{\rm ref}$. Proposed reference values: $\nu_{\rm ref} = 1.5\ \mu{\rm m}^{-1}$ (Marrese & Brown, PM-004), $G_{\rm ref} = 15$ (approximate mid-range), and $T_{\rm ref} = 100$ TDI periods (approximate geometric mean of the minimum and maximum T).

Each FoV/CCD/gate combination requires a different geometric calibration in AGIS, and in the case when the model includes non-geometric effects, these, too, must be different depending on the gate used. Different reference points $G_{\rm ref}$, closer to the actual mean magnitudes, should be chosen for the gated observations.

In the AGIS solution, one should ideally find $c_{\text{non}} = \mathbf{0}$, indicating that the chromaticity and CTI effects have been properly taken into account by the preceding IDU by means of the LSF and CDM calibrations. This will of course never happen in practice. The non-zero chromaticity parameter c_0 can be used to improve the shift parameter h_0 as a function of ν_{eff}, thus providing an *external* LSF calibration to supplement the internal one (cf. footnote 6) or improve the total LSF calibration; however, there is no obvious way to incorporate the non-zero CTI parameters $b_{\alpha\beta}$ into an improved CDM calibration. The non-geometric parameters are therefore mainly *diagnostic* in that they signal some deficiency in the preceding LSF and CDM calibrations.

6.2   Where is the LSF origin set?

In the internal LSF calibration (e.g., as performed in FL) the origin is fixed by the convention $h_0 = 0$. However, this leads in general to $c_{\text{non}} \neq \mathbf{0}$ in the subsequent AGIS solution. Let us assume that we then make a total LSF calibration in the subsequent IDU. If the full calibration vector c from AGIS (including the non-geometric terms) is fed to the FAO calculator in Eq. (22), nothing will be improved in terms of the chromaticity and CDM model. The only way to *force* the LSF calibration in the subsequent IDU to absorb the chromatic shifts, and similarly force the CDM model to produce the proper G and T dependent shifts is by insisting that the calculated LSF origin is achromatic and independent of G and T.

This is done by using only the geometric part η_{geo} when calculating the FAO in Eq. (22). This happens automatically, as the default mode of the FAO calculator is to assume $c_{\text{non}} = \mathbf{0}$. (Only internally in AGIS is the FAO calculator run with the full calibration model, including non-geometric terms.)

As a consequence, the LSF origin obtained in the total LSF calibration corresponds to the centroid for a source with effective wavenumber ν_{ref}. However, in the course of the IDU/AGIS iterations in subsequent processing cycles, the chromaticity becomes fully incorporated in the LSF calibration, eventually resulting in $c_0 \simeq 0$, at which point ν_{ref} loses its meaning.

Similarly, as the CDM calibration improves in the course of the IDU/AGIS iterations, the CTI parameters $b_{\alpha\beta}$ obtained in AGIS gradually diminish in size, until they are negligible; at which point the reference values G_{ref} and T_{ref} lose their meaning.

There is however a subtle difference between how the CDM calibration and the total LSF calibration interacts with AGIS. The CDM model has a built-in capability to 'understand' the case of no radiation damage. Consequently, there is no remaining degeneracy between the purely geometric calibration in η_{geo} and the CDM model. The LSF calibration, on the other hand, has no *a priori* information about what the case of no chromaticity means. Consequently, there remains a degeneracy between the purely geometric calibration in AGIS and the choice of origin in the total LSF calibration. This is potentially problematic when analyzing trends in the various calibrations: an apparent variation of the geometric calibration of AGIS could be caused

by an opposite variation of h_0 in the LSF calibration. It is therefore necessary to introduce the convention that $h_0 = 0$ for a certain reference SED. This is done in Step 5 of the total LSF calibration in Sect. 5.2.

The reference SED must be defined in terms of the colour indices, spectral shape parameters, or whatever spectral data are used to parametrize the LSF calibration. Rather than fixing the reference SED *a priori*, one could use the initial LSF library built during the first several months of the mission (before any AGIS solution can be made) to make a selection that is close to optimal, and which should thereafter not change any more. Since the LSF library is built for photometric classes based on a small number of photometric parameters, one can simply choose a well-populated class in the middle of the photometric parameter ranges.

7 Total PSF calibration

For completeness, the procedure for the total PSF calibration (including AC chromaticity) is here described in analogy with Sect. 5.2:

1. For each image i, the FAO of one sample (k, m) (preferably near the centre of the image) are calculated and the sample is assigned the coordinates $x_{ikm} = D\eta_{ikm}/p_\eta$ and $y_{ikm} = D\zeta_{ikm}/p_\zeta$. The other samples in the image are assigned coordinates that differ by integer values from this. The AC smearing, s, is a known quantity for the image.

2. The counts of each image are flux-normalized: $\hat{N}_{ikm} = N_{ikm}/\sum_{km} N_{ikm}$ (possibly with a correction factor for the flux outside of the window in the AL and AC directions).

3. The PSF parameters h_0, v_0, and h_{nj} (a maximum of $NJ + 1$ parameters) are fitted to the full data set $(x_{ikm}, y_{ikm}, \hat{N}_{ikm})$ using least-squares, chi-square minimization or maximum likelihood.

4. The procedure may be iterated to improve the estimated flux of each image.

5. Re-normalize the PSF calibration by subtracting the (h_0, v_0) estimated for the reference SED (see Sect. 6.2).

8 References

Anderson, J., King, I.R., 2000, PASP, 112, 1360

[UL-031], Lammers, U., 2008, *Proposal of a Generic Astrometric Calibration Scheme for the Data Processing*,
GAIA-C3-TN-ESAC-UL-031,
URL http://www.rssd.esa.int/llink/livelink/open/2817459

[GAIA-LL-044], Lindegren, L., 2003, *Algorithms for GDAAS Phase II - Definition*,
GAIA-LL-044,
URL http://www.rssd.esa.int/llink/livelink/open/357790

[LL-068], Lindegren, L., 2006, *Centroid definition for the Astro line spread function*,
GAIA-C3-TN-LU-LL-068,
URL http://www.rssd.esa.int/llink/livelink/open/2698669

[LL-063], Lindegren, L., 2008, *Geometric calibration model for the 1M astrometric GIS demonstration*,
GAIA-C3-TN-LU-LL-063,
URL http://www.rssd.esa.int/llink/livelink/open/510843

[LL-080], Lindegren, L., 2009, *A framework for consistent definition and use of LSFs in AF/BP/RP/RVS*,
GAIA-C3-TN-LU-LL-080,
URL http://www.rssd.esa.int/llink/livelink/open/2906236

[LL-084], Lindegren, L., 2009, *Minimum-dimension LSF modelling*,
GAIA-C3-TN-LU-LL-084,
URL http://www.rssd.esa.int/llink/livelink/open/2915742

[LL-088], Lindegren, L., 2010, *LSF modelling with zero to many parameters*,
GAIA-C3-TN-LU-LL-088,
URL http://www.rssd.esa.int/llink/livelink/open/3042524

Lindegren, L., 2010, *A posteriori reduction of the set of basis functions for LSF modelling*,
Tech. rep., Lund Observatory,
GAIA-C3-TN-LU-LL-090-01

[PM-004], Marrese, P., Brown, A., 2009, *Describing the BP/RP measurements with spectrum shape coefficients*,
GAIA-C5-TN-LEI-PM-004,
URL http://www.rssd.esa.int/llink/livelink/open/2905783